THE ASTROPHYSICAL JOURNAL, 282:631–640, 1984 July 15

STELLAR WINDS AND MOLECULAR CLOUDS: HERBIG Be AND Ae TYPE STARS

JORGE CANTÓ AND LUIS F. RODRÍGUEZ
Instituto de Astronomía, Universidad Nacional Autónoma de México
NURIA CALVET
Centro de Investigación de Astronomía, Mérida, Venezuela
AND
RUSSELL M. LEVREAULT
Department of Astronomy and Electrical Engineering Research Laboratory,
The University of Texas at Austin
Received 1983 August 5; accepted 1984 February 1

ABSTRACT

We searched for high-velocity carbon monoxide emission in the environments of 11 Herbig Be- and Ae-type stars with the purpose of determining if young stars of intermediate luminosity are commonly associated with molecular outflows, as it is the case for both high- and low-luminosity objects. We detected outflows in LkHα 198 and MWC 1080. The outflow associated with LkHα 198 appears to be bipolar and is of moderate velocity. MWC 1080 exhibits a powerful, apparently isotropic outflow that affects a considerable fraction of the parent cloud. The CO line wing emission extends over at least 25 km s^{-1}. We estimate the stellar mass loss rate of MWC 1080 to be of the order of 10^{-5} $M_{\odot}$ yr^{-1}. Analysis of optical and infrared data suggests a correlation between abundant circumstellar material and detectable molecular outflows.

Subject headings: radio sources: lines — stars: circumstellar shells — stars: emission-line — stars: mass loss — stars: pre–main-sequence — stars: winds

I. INTRODUCTION

During the last few years it became evident that the effects of a stellar wind from a recently formed object on the surrounding molecular gas could be studied by radio observations of carbon monoxide and other molecules. The gas accelerated by the stellar wind is apparent in the CO line as wings or bumps displaced in radial velocity from the emission of the ambient cloud. The presence of this high-velocity molecular gas provides evidence for the existence of a stellar wind, regardless of the ambiguities of the optical line profile interpretation and also allows an approximate determination of the wind parameters.

Most of the work has concentrated on the environment of heavily obscured OB stars (Zuckerman, Kuiper, and Rodríguez Kuiper 1976; Kwan and Scoville 1976; Rodríguez *et al.* 1982; Bally and Lada 1983), and of visible T Tauri stars (Kutner *et al.* 1982; Edwards and Snell 1982; Calvet, Cantó, and Rodríguez 1983). One important general result of that research has been that pre–main-sequence stellar winds appear to be more powerful than main-sequence ones. We considered important to search for high-velocity CO emission in the vicinity of young stars of intermediate mass to that of OB stars ($M_* \gtrsim 10\ M_{\odot}$) and T Tauri stars ($M_* \lesssim 2.5\ M_{\odot}$). However, to produce abundant high-velocity molecular gas one requires the presence both of a strong stellar wind and of an associated molecular cloud. These ideas pointed naturally to the group of Be- and Ae-type stars associated with nebulosity, first discussed by Herbig (1960). These stars have been interpreted as young objects (Strom *et al.* 1972), and thus they are expected to possess strong winds. In this paper we present carbon monoxide observations of the molecular environments of 11 stars selected from the 26 stars in Herbig's catalog. In § II we describe the observations, while in § III we comment on the properties of each individual source derived from optical and radio observations. Based on this compilation, we present a general discussion in § IV. Finally, we summarize our results and give our conclusions in § V.

II. OBSERVATIONS

Eleven Be- and Ae-type stars associated with nebulosity were selected as sources. From the list of Herbig (1960) we took out those stars associated with blue and smoothly shaped nebulae, assuming them to be classical reflection nebulae. We were left with 10 stars associated with a nebulosity that was either red or of irregular shape. We tentatively assumed these cases to be either shocked gas or ejecta from the star. Finally, we also included in our list LkHα 208, which is associated with a bipolar reflection nebula of characteristics somewhat similar to those of NGC 2261, a source with observed bipolar outflow (Cantó *et al.* 1981). The illuminating star of NGC 2261, R Mon, is also included in Herbig's list. The 11 stars observed are listed in Table 1. Most of the stars in Herbig's catalog were already surveyed in CO with a moderate angular resolution of 2′.6 by Loren, Vanden Bout, and Davis (1973).

The $J = 1 \rightarrow 0$ observations of CO and ^{13}CO were made during 1981 September 14–18, using the 11 m radiotelescope of the National Radio Astronomy Observatory[1] at Kitt Peak, Arizona. We used the cooled 80–120 GHz mixers with orthogonally polarized feeds without Fabry-Pérot image rejection filter. The data were calibrated using the chopper wheel technique and comparing with standard sources (Ulich and Haas 1976). The system temperature was typically in the range 2000–2500 K for CO and 1200–1600 K for ^{13}CO. Each linear

[1] The NRAO is operated by Associated Universities, Inc., under contract with the National Science Foundation.

TABLE 1

OBSERVED Ae AND Be STARS

STAR	CENTRAL POSITION[a] α(1950)	CENTRAL POSITION[a] δ(1950)	REFERENCE POSITION α(1950)	REFERENCE POSITION δ(1950)	l^{II}(°)	b^{II}(°)	DISTANCE[b] (kpc)	LUMINOSITY[b] ($L_\odot$)	SPECTRUM[b]	$A_v^{op\ b}$
LkHα 198	00ʰ08ᵐ47ˢ.5	58°33′06″	00ʰ16ᵐ26ˢ.8	58°33′06″	117.8	−3.6	1.0	1×10^3	B3	4.5
AB Aur	04 52 34.2	30 28 22	04 57 12.7	30 28 22	172.5	−8.0	0.14	100	A0	0.7
RR Tau	05 36 23.5	26 20 50	05 36 23.5	25 20 50	181.5	−2.5	0.8	130	A6	0.8
HD 250550	05 59 06.5	16 31 06	05 54 56.2	16 31 06	192.6	−3.0	0.28	33	B6	0.02
LkHα 208	06 04 53.2	18 39 55	06 13 19.7	18 39 55	191.4	−0.8	1.0	100	F0	0.4
Z CMa	07 01 22.6	−11 28 36	07 01 22.6	−13 28 36	224.6	−2.6	1.15	1.4×10^3	B8	3.5
HD 53367	07 02 03.9	−10 22 23	06 57 59.9	−10 22 23	223.7	−1.9	1.2	2.5×10^4	B0	2.1
MWC 297	18 25 02.2	−03 53 16	18 08 59.9	01 53 16	26.8	3.5	0.45	...	B	...
BD +40°4124	20 18 45.5	41 12 27	19 52 15.5	41 12 27	78.9	2.8	2.0	2.9×10^3	B2	3
LkHα 233	22 32 30.3	40 23 28	22 32 30.3	42 23 28	96.7	−15.2	0.9	120	A7	2.6
MWC 1080	23 15 16.3	60 33 52	00 03 48.4	60 34 22	111.7	0.0	2.5	1.7×10^4	B0(c)	5.4

[a] The central positions may differ slightly from more recent determinations of the position of the star.

[b] See discussion in § III.

polarization fed one-half of the two filter banks used (100 kHz and 500 kHz), and the halves of each filter bank were averaged resulting in spectra of 128 channels and velocity resolutions of 0.26 and 1.30 km s^{-1} for CO and 0.27 and 1.36 km s^{-1} for ^{13}CO. The data were taken by position switching every minute against a reference position checked previously to be free of CO emission to a 4 σ level of $\sim$0.5 K. The source and reference positions are given in Table 1. Adopted distances, luminosities, spectral types, and visual extinctions, are also given in this table; these parameters are further discussed in § III. All sources were observed in CO within a 3 × 3 grid with elements separated 60″, approximately one full beamwidth (66″ at the CO frequency). When the surrounding cloud showed evidence of localized kinematic activity, data were taken at half-beamwidth intervals to fill the grid, and in other cases the mapping was extended out considerably as described in § III. The criteria used to establish if there are ordered high-velocity molecular motions were those described in Calvet, Cantó, and Rodríguez (1983). They are: (1) the full width at zero power of the wings should be $\gtrsim$10 km s^{-1}; (2) the full width at zero power of the wings should be greater than 3 times the full width at half-power of the main line emission; (3) the total emission profile should be relatively simple; and (4) the wing emission should diminish in intensity as we move a few arc minutes away from the central star. It should be pointed out, however, that these criteria could lead to missing cases of either low-velocity or very extended outflows, which require a more detailed study of the region. The ^{13}CO, $J = 1 \rightarrow 0$ transition was observed only at the central position. The CO and ^{13}CO spectra taken at the central position with the 100 kHz filter bank are shown in Figure 1. We deleted three channels at each end of the ^{13}CO spectra and stretched them to align in velocity space with the CO spectra. In Table 2 we give the parameters of the CO and ^{13}CO spectra obtained at the central position, as well as the molecular hydrogen column density and the corresponding visual extinction derived from the formulation of Dickman (1978). In this table we also list the estimated angular and physical diameter, H_2 density, and mass of the directly associated molecular cloud. These two latter parameters were estimated assuming that the cloud is a constant density sphere.

At one position in one object (MWC 1080), $J = 2 \rightarrow 1$ observations were obtained with the MWO[2] 4.9 m radiotelescope

[2] The Millimeter Wave Observatory is operated by the Electrical Engineering Research Laboratory, the University of Texas at Austin, with support from the National Science Foundation and McDonald Observatory.

TABLE 2

OBSERVED AND DERIVED PARAMETERS FOR THE ASSOCIATED CLOUDS

STAR	CO EMISSION[a] T_{peak} (K)	CO EMISSION[a] Δv (km s^{-1})	CO EMISSION[a] V_{LSR} (km s^{-1})	^{13}CO EMISSION[a] T_L (K)	^{13}CO EMISSION[a] Δv (km s^{-1})	^{13}CO EMISSION[a] V_{LSR} (km s^{-1})	$N(H_2)$ (10^{21} cm^{-2})	A_v (mag)	θ_s (arcmin)	L (pc)	$n(H_2)$ (cm^{-3})	M ($M_\odot$)
LkHα 198	11.4	2.6	−0.7	3.8	1.7	−0.1	4.4	3.5	12	3.5	410	450
AB Aur	12.4	1.0	6.1	3.9	0.5	6.0	1.4	1.1	~10	0.4	1100	2
RR Tau	11.2	1.3	−5.4	3.0	0.8	−5.4	1.6	1.2	5	1.2	430	20
HD 250550	6.2	2.1	2.1	1.5	1.1	2.3	0.9	0.7	5	0.4	730	1
LkHα 208	9.6	1.6	0.1	2.5	1.4	−0.5	2.1	1.7	14	4.1	170	300
	2.0	1.3	3.5	0.3	0.5	3.6	0.1	0.1	...	...	...	...
Z CMa	12.5	2.3	13.9	4.0	1.3	13.9	3.7	2.9	8	2.7	450	260
HD 53367	12.9	3.6	18.7	4.2	2.5	17.3	7.5	6.0	8	2.8	860	500
MWC 297	4.9	3.6	4.1	2.6	2.2	5.6	3.7	2.9	~30	3.9	300	500
	3.7	2.9	12.4	1.3	2.1	10.9	1.5	1.2	...	...	...	...
BD +40°4124	19.7	2.3	7.9	6.3	1.6	7.7	9.1	7.3	6	3.5	840	900
	8.3	1.3	12.8	2.0	0.8	12.8	0.9	0.7	...	...	...	...
	3.8	1.3	14.2	0.5	0.8	14.1	0.2	0.2	...	...	...	...
	2.3	3.1	2.2	<0.5	...	...	...	...	...	...	...	...
LkHα 233	13.6	1.3	0.1	4.5	0.8	0.0	2.7	2.1	6	1.5	580	50
MWC 1080	8.8	8.9	−29.1	2.8	2.7	−30.6	4.6	3.7	6	4.4	340	800

[a] At the central position given in Table 1.

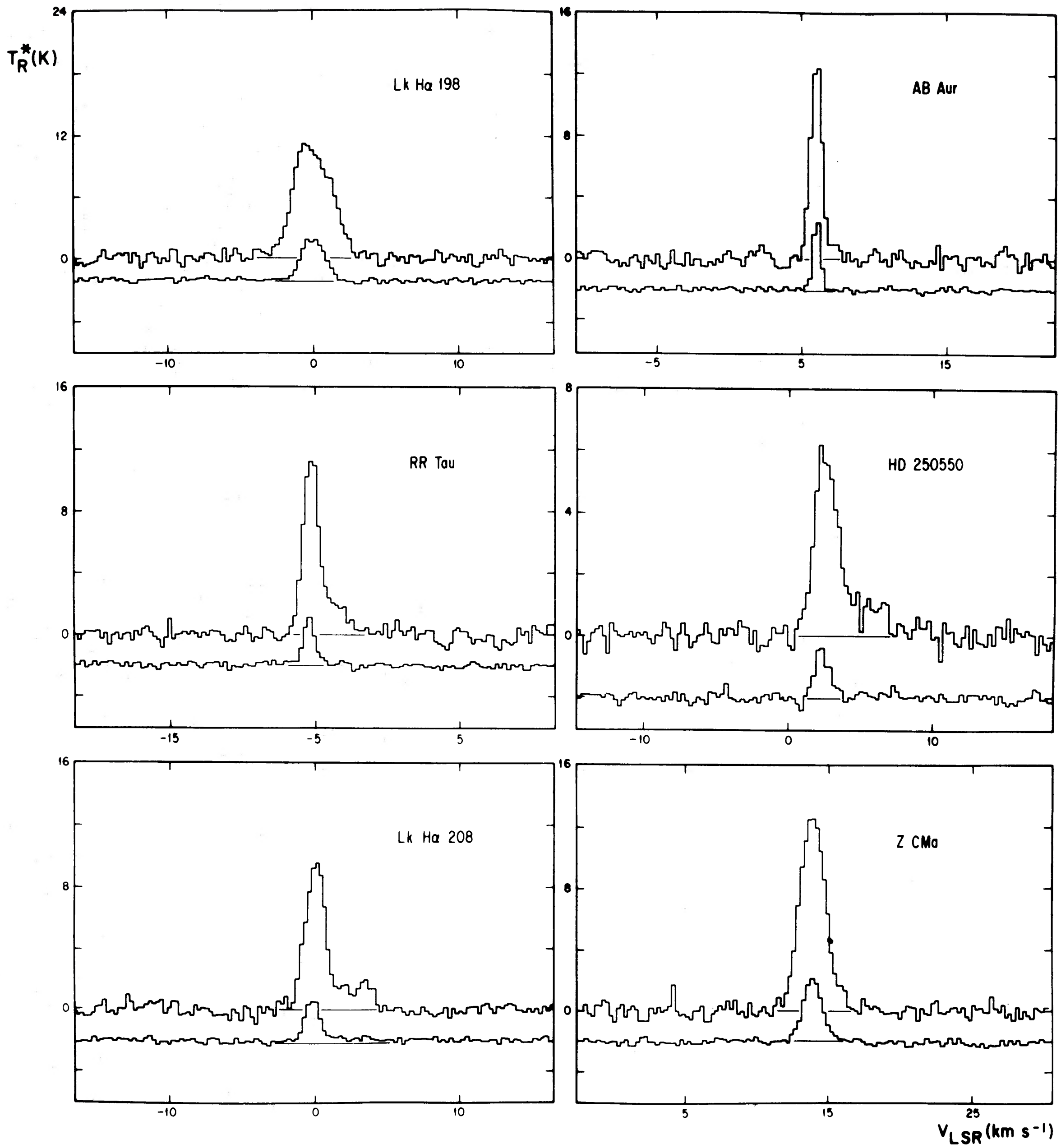

FIG. 1.—Spectra of CO (*top*) and ^{13}CO (*bottom*) for the central positions observed. The source antenna temperature, T_R*, is defined by Kutner and Ulich (1981). The velocity resolutions are 0.26 km s^{-1} for CO and 0.27 km s^{-1} for ^{13}CO.

during 1982 March. The equipment and data acquisition techniques were those described by Levreault (1983).

III. COMMENTS ON INDIVIDUAL SOURCES

a) *LkHα 198*

A spectral type of Ae was assigned to this star by Herbig (1960), and later Cohen (1975) reported its spectrum as strongly "veiled." However, Cohen and Kuhi (1979, hereafter CK) were able to classify it as B3, using the strength of the He I absorption lines. They determined $A_v = 4.5$ mag from the continuum slope. From the ratio of Hα/Hβ observed (CK) one can obtain $A_v = 8.5$ mag assuming that the ionization is purely radiative and a standard reddening law. This much larger value for A_v suggests that the intrinsic Hα/Hβ may be larger. This could be expected if the excitation is collisional in nature (Gerola, Salem, and Panagia 1971), hinting at the presence of a wind. We adopt a distance of ~1.0 kpc based on the photometry and spectroscopy of three nearby stars that illuminate reflection nebulae given by Herbig (1960).

We have taken ^{12}CO observations at the central position (Fig. 1) and at 26 positions around it, covering a region of ~5′ × 5′. The observations show a main line centered at $V_{LSR} \approx -0.7$ km s^{-1}. The spectra also show a blue wing to the NW of the star and a red wing to the SE, as shown in Figure 2. Figure 3 shows contours of integrated T_R* over radial velocity for the blue and red emissions. The blue wing was integrated from −4.7 to −1.5 km s^{-1} and the red wing from 0.7 to 3.9 km s^{-1}.

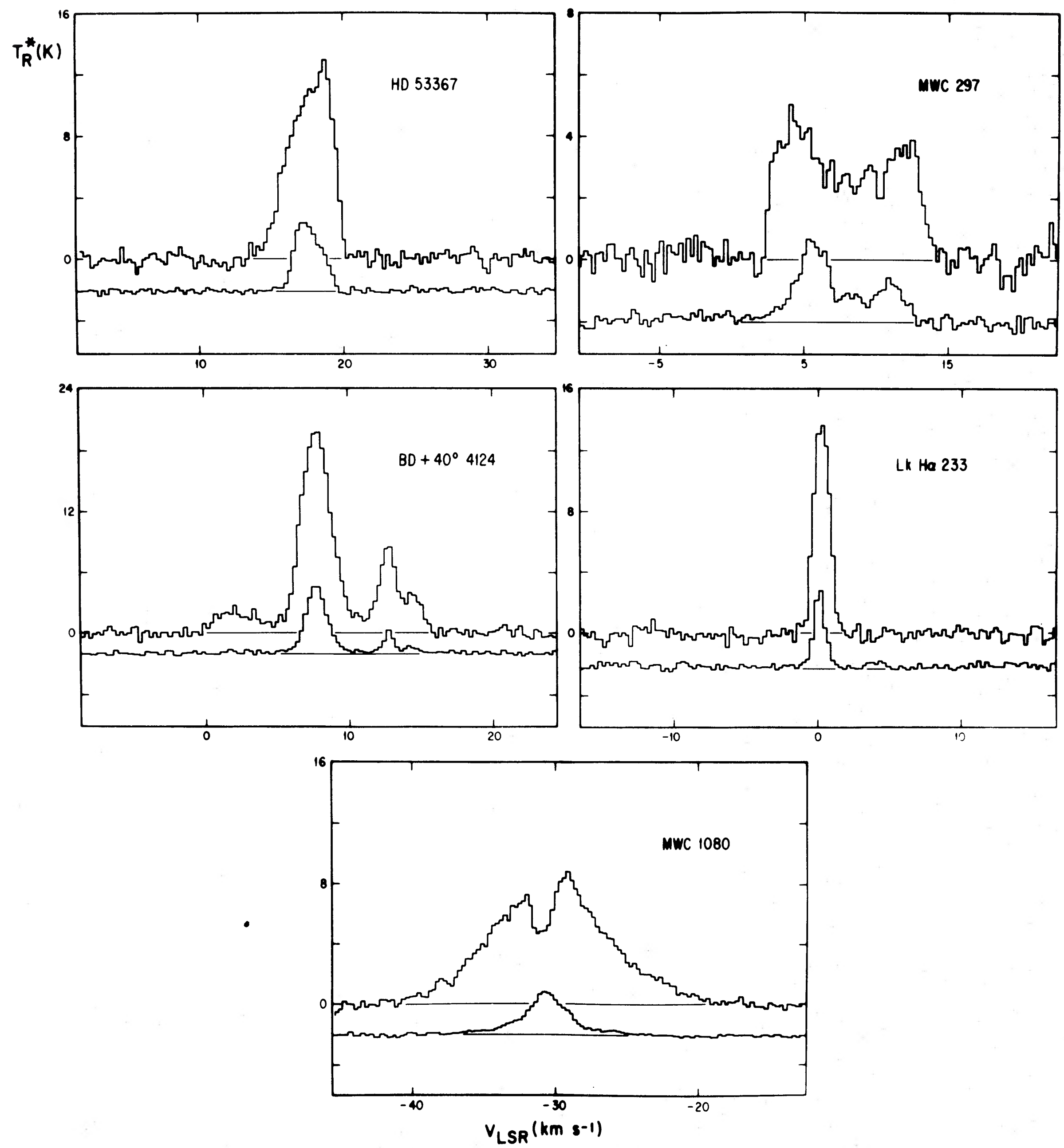

FIG. 1.—*Continued*

Although the lobes are not symmetric with respect to the star, we interpret these observations in terms of a bipolar outflow, similar to those observed in other types of objects. This bipolar outflow was independently detected by Bally and Lada (1983). The bipolar outflow in LkHα 198 covers a range of ~ 8 km s^{-1} in radial velocities, a comparatively modest value. The outflow is oriented in the NW-SE directions and covers an extended region of $\sim 4' \times 2'$ with a separation between the maxima of $\sim 1\overset{'}{.}5$ (Fig. 3). The optical nebulosity (see Fig. 1 in Herbig 1960) is to the SE of the star and may be associated with the receding material. We give in Table 3 the outflow parameters, calculated following Calvet, Cantó, and Rodríguez (1983).

Contours of antenna temperature at fixed V_{LSR} show the existence of two maxima of temperature: (*a*) $T_R{}^* = 22$ K, located at $\Delta\alpha = 0'$, $\Delta\delta = 2\overset{'}{.}5$ from the star with $V_{LSR} = -0.52$ km s^{-1}, and (*b*) $T_R{}^* = 17$ K, at $\Delta\alpha = -1\overset{'}{.}5$, $\Delta\delta = 3'$, with $V_{LSR} = 0.26$ km s^{-1}. These two maxima were already found by Loren (1977). Loren's maximum at the north of the star is consistent in position with maximum (b). However, we find a difference in position of $\sim 2'$ between Loren's south maximum and our maximum (a). The maxima do not seem to be associated in any obvious way with the bipolar outflow. There is an angle of $\sim 30°$ between a line joining maxima (a) and (b) and the symmetry axis of the bipolar flow. Moreover, the V_{LSR}'s from the main line for the two maxima are in opposite sense to

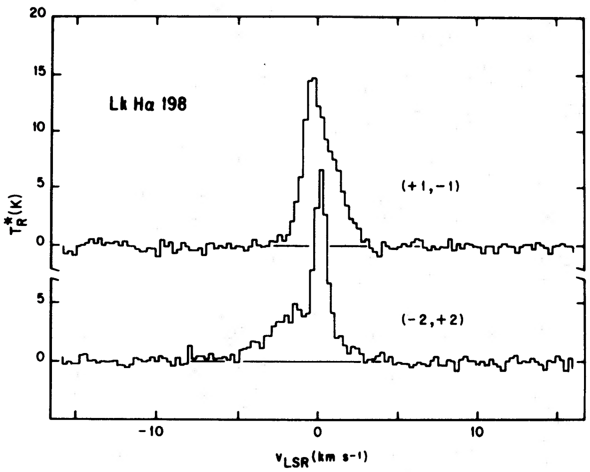

FIG. 2.—Carbon monoxide spectra at two positions near LkHα 198 showing redshifted (*top*) and blueshifted (*bottom*) wing emission. The numbers in parentheses are the offsets in right ascension and declination from the central position given in arc minutes.

the velocities of the outflow indicated by the wings. We conclude that the two temperature maxima correspond to two independent clouds or temperature enhancements in the region.

b) AB Aurigae

According to Herbig (1960), the spectrum of this star corresponds to that of a B9 star plus a weak absorption shell. CK classified it as B9–A0, with total luminosity of 10^2 $L_\odot$, corresponding to a luminosity class either IV or V. Felenbok, Praderie, and Talavera (1983) interpret the optical spectrum as indicative of the presence of a wind. The star is located near the edge of an irregular and extended molecular cloud of about 10′ × 10′ in angular size.

The CO emission line in the direction (Fig. 1) and vicinity of AB Aur shows no obvious signs of high-velocity gas motions. The emission lines are quite narrow with a full width at half-maximum of ~0.9 km s^{-1}. There is, however, a slight indication of gas moving at moderate velocity in the form of a small pedestal at the red side of the main line. This emission can also be seen in the spectra taken 1′ north, west and south of the star, suggesting it comes from an unrelated molecular cloud.

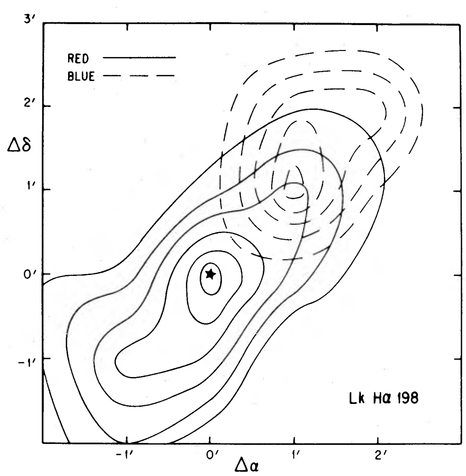

FIG. 3.—Contour map for the velocity-integrated red and blue CO wings in LkHα 198. The lowest contour is 6 K km s^{-1} and increments are in units of 1 K km s^{-1}. The redshifted emission was integrated over the velocity interval from 0.7 to 3.9 km s^{-1} and the blueshifted emission from −4.7 to −1.5 km s^{-1}.

Adopting a distance of 140 pc for AB Aur (the same as that of the Taurus-Aurigae molecular complex; Elias 1978) and a cloud angular diameter of ~10′, the molecular hydrogen column density of Table 2 implies an average density of ~10^3 cm^{-3}. The associated cloud mass is then ~2 $M_\odot$. These two values are most likely to be strong lower limits since the star is located at the edge of the cloud where the density is likely to be much smaller.

Contours of T_R^* (max) show a temperature peak of 12 K at the star's position. This heating could be produced by the radiation from AB Aur if $n_{H_2} \approx 4 \times 10^3$ cm^{-3} (Loren and Wootten 1978; Goldsmith and Langer 1978). This density is only a few times higher than the lower limit estimated previously, suggesting that radiative heating is a plausible mechanism for the molecular gas in the vicinity of AB Aur.

c) RR Tauri

Early work by Herbig (1954) classified this star as an A2 II–III. However, later spectroscopic results, also by Herbig (1960), indicate RR Tau to be more probably a B8–B9 star plus a shell. More recently, CK give a spectral type of A6 which we adopt.

We have taken CO spectra of RR Tau in a 3′ × 3′ grid around the central position and at four more points to the SW of the star. The source antenna temperature drops rapidly to the west of the star and the contours follow the boundary of the associated dark cloud.

The distance to RR Tau is not known. However, if we assume that the star is at the same distance as the neighboring star BD +26°887, which has a distance modulus of 9.5 mag (Herbig 1960), we obtain a value of about 800 pc.

d) HD 250550

This star has been classifed as B8 (T_{eff} = 12,000 K) by Strom *et al.* (1972) and as B6 by CK. Data in Table 2 are taken from the latter authors. Herbig (1960) reports strong emission at Hα and Hβ but weak Hγ, in agreement with CK. P Cygni structures in the Balmer lines have been observed by Herbig (1960) and Garrison and Anderson (1977). In addition, Garrison (1978) finds flux excesses at the Balmer and Paschen discontinuities. These observations can be interpreted in terms of an ionized wind flowing out from the star. In fact, Garrison (1978) estimates $\dot{M} \approx 0.7\text{–}3 \times 10^{-7}$ $M_\odot$ yr^{-1}.

The star is associated with an arc of reflection nebulosity located to the NE. This arc is located ~24″ from the star (see Herbig 1960, Fig. 2). In turn, the arc is surrounded by a fainter nebulosity. The system is located in a cloud ~5′ in diameter. We have two estimates for the distance to the star. The kinematic distance corresponding to the V_{LSR} of the ^{13}CO is 0.39 kpc. Strom *et al.* (1972) find a spectroscopic luminosity of 32 $L_\odot$, based on their determination of log g and T_{eff} from the spectrum. This luminosity can be combined with the value of $L/D^2 = 4.16 \times 10^{-4}$ $L_\odot/pc^2$ from CK to give a distance of 0.28 kpc in good agreement with the kinematic distance. We adopt the spectroscopic determination.

We have taken CO spectra at 14 points at and around the star position. The peak source antenna temperature shows a maxima of 6.2 K at the central position. However, there is evidence of peculiar activity in the direction of the arc-shaped nebulosity. First, the T_R* contours are elongated toward the NE, in the direction of the optical arc. Second, there is a velocity gradient of ~0.34 km s^{-1} per arcmin (4.2 km s^{-1} per pc) at 20° p.a. approximately parallel to the line joining the star and the center of the arc.

e) LkHα 208

The optical appearance of the associated nebula strongly suggests the presence of a disk of material around the central star (see Fig. 8 in Herbig 1960). We have taken CO spectra in a 3′ × 3′ grid around the star. The observation at the central position encompasses the central star and most of the optical nebulosity. The observed CO emission shows an increase in source antenna temperature toward the east, almost certainly due to the molecular cloud at which edge LkHα 208 lies (see POSS plates).

The CO and ^{13}CO profiles show two peaks, corresponding to $V_{\rm LSR} = 0.1$ km s^{-1} and $V_{\rm LSR} = 3.5$ km s^{-1}. For both components the peak antenna temperature increases towards the east, and this effect is noticeable both in CO and ^{13}CO. We interpret these components as produced in two different clouds located along the line of sight toward the star. We associate LkHα 208 with the cloud producing the strongest feature (at 0.1 km s^{-1}) since to produce a reflection nebula a large amount of gas around the star is required. The interstellar reddening versus distance diagrams of Fitzgerald (1968) suggest that this star is at ~1 kpc. We adopt this distance as a crude estimate.

f) Z CMa

There is considerable uncertainty on the spectral type of the star. CK classify it as an F star. However, on the basis of analysis of the He I lines, Strom *et al.* (1972) assign a $T_{\rm eff} =$ 12,000 K, corresponding to a B8 star. The reddening determination is also quite uncertain. CK give $A_v = 2.82$, and Strom *et al.* (1972) give a color excess of $E(B-V) = 1.14$, corresponding to $A_v = 3.5$, with a standard reddening law. These differences could be due to intrinsic variability of the star, as mentioned by Herbig (1960). We will adopt the value of $A_v = 3.5$ from Strom *et al.* (1972). We have also adopted a distance to the star of 1150 pc, since it is a member of the CMa R1 association (Herbst, Racine, and Warner 1978). The Hα line of Z CMa shows a classical P Cygni profile (Finkenzeller and Mundt 1984), which suggests the presence of a wind.

The CO lines at all positions of the 3′ × 3′ grid are approximately Gaussian in shape. The contour map of maximum line antenna temperature shows lines running along the EW direction with the greatest temperature along the line passing through the star's position. However, the temperature is enhanced by 1–2 K in two regions displaced symmetrically in right ascension by ~1′ from the star. Our observations did not extend far enough to determine how large these regions of enhanced temperature are. We also note that the velocity of the peak of the main line increases towards the west, from which we infer a velocity gradient in the cloud of 0.26 km s^{-1} per arcmin or of 0.78 km s^{-1} per pc, at the adopted distance. The two symmetric peaks in antenna temperature and the velocity gradient could be interpreted in terms of an interstellar disk rotating around the star. This hypothetical disk would be consistent with the large reddening observed towards the star.

g) HD 53367

Herbig (1960) assigns to this star a type of B0 IV and reports that no spectral change took place between 1920 and 1960. However, the star has recently shown signs of activity, both in the lines (Hubert-Delplace and Hubert 1979) and in the continuum (Schuster 1984). It is not clear whether or not the star has a wind, since although Hα is broad, it does not appear to have an absorption feature (Garrison and Anderson 1977) and the broadening could be due to rotation. Strom *et al.* (1972) estimate a color excess of $E(B-V) = 0.7$ for this star, from which $A_v = 2.1$, using a standard reddening law. The star is centered in the bright nebula IC 2177 and is surrounded by an arc of dark material running E-W (see Fig. 8 in Herbig 1960).

We have taken ^{12}CO observations at the central position (Fig. 1) and at 16 other positions around it. Contours of source antenna temperature in a diagram of declination versus radial velocity show two clearly distinct components as can be seen in Figure 4. The component with $V_{\rm LSR} \sim 17$ km s^{-1} extends toward the south, while the component with $V_{\rm LSR} \sim 19$ km s^{-1} extends toward the north. A comparison of the spectra of CO and ^{13}CO at the central position (Fig. 1) indicates that the component with $V_{\rm LSR} \sim 19$ km s^{-1} is hotter and has less column density than the component at 17 km s^{-1}. We find that the CO lines coming from the same declination and symmetrically displaced in α from the central position are very similar. Based on this fact and on the presence of the two velocity components, we interpret the CO observations in terms of a model consisting of a toroid surrounding the star and expanding at a velocity of about 1 km s^{-1}. It is interesting that the toroidal morphology is clearly suggested by the optical appearance of the surrounding dark arc (Fig. 8 of Herbig 1960). Consistently with this interpretation, the spectra obtained east and west of HD 53367 peak at a velocity of ~18 km s^{-1}. Similar toroidal structures of interstellar dimensions have been found around many other young stellar objects (Little *et al.* 1979; Cantó *et al.* 1981; Bally and Scoville 1982; Torrelles *et al.* 1983).

The distance to HD 53367 is not known. However, we can take the systemic $V_{\rm LSR} \sim 18$ km s^{-1} and infer from it a kinematic distance of 1.2 kpc, which we adopt.

h) MWC 297

Very little information exists for the optical spectrum of this star. Herbig (1960) describes it as a B-type star with strong emission in Hα and Hβ. The steep Balmer decrement indicates that the absorption is large and that probably the star is deeply embedded in the cloud. The infrared spectrum of the star can

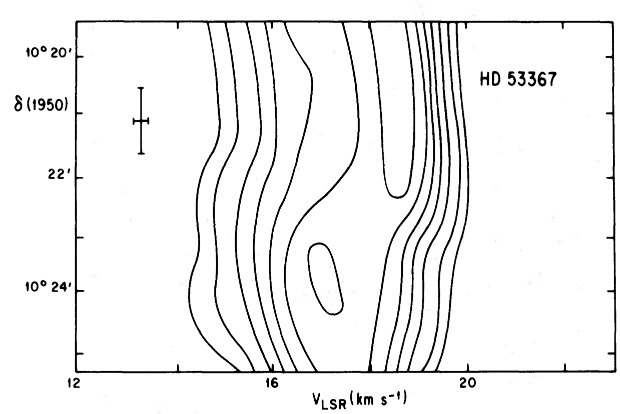

FIG. 4.—Contour diagram of velocity vs. declination for the CO emission associated with HD 53367 at α(1950) = 07$^{\rm h}$02$^{\rm m}$03$^{\rm s}$.9. The contour levels are 1, 2, 4, 6, 8, 10, and 12 K. The cross defines the angular and spectral resolutions.

be explained as thermal emission by dust (Cohen 1975), which indicates that part of the reddening must be circumstellar.

The CO spectra are very complex, showing two components at $V_{\mathrm{LSR}} \approx 4.1$ km s^{-1} and $V_{\mathrm{LSR}} \approx 12.4$ km s^{-1} (Fig. 4). There is no clear pattern in the spatial distribution of these components, suggesting two independent clouds.

The V_{LSR} velocities of the ^{13}CO emission from the two clouds correspond to kinematic distances of 0.45 and 0.87 kpc. We assign to MWC 297 the kinematical distance of the cloud with highest temperature in CO, namely 0.45 kpc. Kinematic distances smaller than ~ 1 kpc are not reliable, thus we consider this distance as a crude estimate.

i) BD +40°4124

The spectral type of the star is estimated as O9.5 V by Herbig (1960) and as B2 by Strom *et al.* (1972), with corresponding reddenings of 3.3 and 3.1 mag. The Hα emission profile shows an unshifted central absorption component (Herbig 1960; Garrison and Anderson 1977). This can be understood in terms of rotation alone, but a model consisting of a dense rotating and expanding envelope may also be appropriate (cf. Marlborough 1970). Thus, the presence of a stellar wind cannot be discarded.

We adopt Herbig's (1960) estimate for the distance to the star, $D = 2$ kpc. The star is embedded in a region delineated by a bright rim, except in the north side. This rim is specially bright in the east side. The nebulosity immediately surrounding the star is probably produced by reflection (Herbig 1960).

We have taken CO spectra at the central position (Fig. 1) and at 16 points around the star, covering a region of $\sim 4'$ in size. The spectra are very complex. They show four components at $V_{\mathrm{LSR}} = 2.2$, 7.9, 12.8, and 14.2 km s^{-1}. A map of the most intense component, that corresponding to 7.9 km s^{-1}, matches the optical appearance of the system and strongly suggests that this cloud is a protuberance of the larger molecular cloud located north of BD +40°4124. This protuberance shows a maximum temperature of ~ 23 K coincident, within our pointing accuracy ($\sim 15''$), with the optical position of the star, $\alpha(1950) = 20^{\mathrm{h}}18^{\mathrm{m}}42\overset{\mathrm{s}}{.}2$; $\delta(1950) = 41°12'15''$ (Della Prugna 1982).

It is not clear if the other clouds ($V_{\mathrm{LSR}} = 2.2$, 12.8, and 14.2 km s^{-1}) are related to BD +40°4124. It is interesting, however, that the clouds at 2.2 and 14.2 km s^{-1} have maxima nearly coincident in space, at position $(\Delta\alpha, \Delta\delta) = (1', 1')$, from the adopted central position (Table 1). Moreover, their V_{LSR} are ± 6 km s^{-1} different from the V_{LSR} of the main cloud. One could thus argue that these two clouds are spatially related to the main cloud, although the actual relationship is not clear. This source requires a more detailed study.

j) LkHα 233

The spectral type of the star is estimated as A7 (Herbig 1960) and its reddening as 2.6 mag (Calvet and Cohen 1978).

We have taken CO spectra at the central position (Fig. 1) and at 16 other positions covering a region of $\sim 2'$ in size. The spectra show a narrow main line at all positions. Contours of T_R^* (max) show no obvious heating associated with the star but instead an increase of ~ 6 K in antenna temperature from E to W. This gradient is probably associated with the main cloud complex. Contours of T_R^* in position versus velocity show a velocity gradient of ~ 0.22 km s^{-1} per arcmin in the direction 60° p.a. At the distance of 0.9 kpc (Calvet and Cohen 1978), this gradient corresponds to 0.84 km s^{-1} per pc. The position angle of the velocity gradient agrees with the axis of symmetry of the bipolar nebulosity. Thus, the gradient could be due to a low-velocity bipolar flow, since the fainter lobe (NE), tentatively identified as the obscured lobe, corresponds to redshifted material. Alternatively, the velocity gradient may not be directly related to the star but to the molecular cloud as a whole, since it is small and does not seem to be confined to the lobes, but extends continuously over the mapped area. With the present observations, we cannot discriminate between the two alternatives.

k) MWC 1080

No spectral classification was assigned by Herbig (1960) to MWC 1080. CK classified it as a B0 using the strength of the He I absorption lines, although they added the designation (c) because no other absorption features could be seen. The spectrum shows strong emission lines of Fe II and resembles that of the most active T Tauri stars, except for the He I lines. CK finds $A_v = 5.42$ mag using their continuum indexes. Strong P Cygni absorptions in the Balmer lines are reported by Herbig (1960), Garrison and Anderson (1977), and Finkenzeller and Mundt (1984).

Using the value for L/D^2 given by CK and the luminosity of a ZAMS B0 star from Panagia (1973) we obtain a photometric distance of 3 kpc. On the other hand, from the V_{LSR} of the ^{13}CO emission from the main cloud, we obtain a kinematic distance of 2.5 kpc. If the star were one subclass later (a possible situation since CK's classification scheme is accurate within one subclass), both estimates of distances would agree. We choose then to adopt the kinematic value of 2.5 kpc.

We took CO observations at the central position (Fig. 1) and at 40 other positions around the star. The CO lines show strong self-absorption and broad wings, extending ~ 25 km s^{-1} in radial velocities at either side of the main line for the central position (Fig. 1). The wings are also present in the ^{13}CO spectrum taken at the central position. Figure 5 shows contour maps of integrated source antenna temperature in the wings, over an area of $5' \times 5'$ around the star. The blue wing was integrated from $V_{\mathrm{LSR}} = -43.2$ to -32.8 km s^{-1}, and the red wing from -27.6 to -17.2 km s^{-1}. The inner values of these

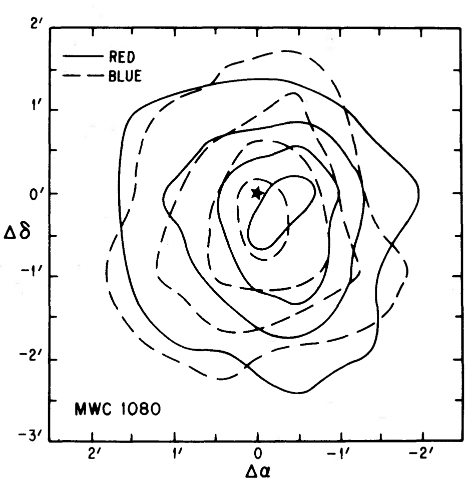

FIG. 5.—Contour map for the velocity integrated red and blue CO wing emission in MWC 1080. The lowest contour is 5 K km s^{-1}, and increments are in units of 5 K km s^{-1}. The redshifted emission was integrated from -27.6 to -17.2 km s^{-1}, while the blueshifted emission was integrated from -43.2 to -32.8 km s^{-1}.

intervals were taken to be equal to those where the ^{13}CO wings start to appear. Spectra taken away from the high-velocity region indicate that there is no significant contribution of the ambient cloud in these velocity intervals. The redshifted and blueshifted emissions are produced in extended regions, about 2′–3′ across, which are spatially coincident within observational errors and have their maxima at the star position, $\alpha(1950) = 23^h15^m14^s.45$; $\delta(1950) = 60°34'21''.1$ (Cova *et al.* 1984). Also, the peak of antenna temperature coincides with this position. Outflows with spatially coincident blueshifted and redshifted regions of emission can be interpreted as due either to an isotropic outflow or to a bipolar outflow observed along its axis. However, the absence of a high-density region around the star that could act as a focusing mechanism for the stellar wind (Torrelles *et al.* 1983) favors the isotropic possibility. We estimate an angular diameter of $\sim 6'$ for the associated molecular cloud. The sizes inferred above for the regions where the wing emission is present indicate that the outflow phenomenon is affecting considerably the parent cloud.

The parameters of the outflow are given in Table 3. As in most of the outflow cases (e.g., Rodríguez *et al.* 1982; Bally and Lada 1983), the mechanical momentum rate in the outflow exceeds by about an order of magnitude the available radiative momentum rate, L_*/c. From the derived momentum rate, and assuming a terminal velocity for the wind of 200 km s^{-1}, we obtain a stellar mass loss rate of $\dot{M} \sim 10^{-5}\ M_\odot$ yr^{-1}. The outflow associated with MWC 1080 is one of the most massive yet detected and one of the few related to a visible object.

The 500 kHz filter bank spectra show the presence of a cloud at $V_{LSR} \approx -47$ km s^{-1} located to the SE of the cloud associated with MWC 1080. This other cloud is probably much more distant and is not evident in the POSS plates.

Finally, given the velocity extent of the high-velocity CO emission, we considered valuable to obtain a $J = 2 \rightarrow 1$ spectrum at the central position with a similar beam size to obtain information on the excitation temperature of the gas as a function of radial velocity (Loren *et al.* 1981). The ratio, $R_2 = T_R$ $(J = 2 \rightarrow 1)/T_R$ $(J = 1 \rightarrow 0)$, for CO as a function of radial velocity with respect to the LSR is shown in Figure 6. T_R is the source radiation temperature as defined by Kutner and Ulich (1983) and has been obtained from the MWO and Kitt Peak data assuming a source angular diameter of 4′ and following Levreault (1983). The ratio is ~ 1 within the main line but rises to 2–3 in the line wings. This is similar to what is observed in other wing sources (Loren *et al.* 1981; Levreault 1983; Plambeck, Snell, and Loren 1983). If the transitions from the high-velocity gas are thermalized, this result implies that this gas is either moderately thick and clumpy, or optically thin and cooler than the gas from the main cloud. Plambeck, Snell, and Loren (1983) favor the first possibility. However, if the transition is not thermalized, one can reach different conclusions. The lack of detectable NH_3 emission in MWC 1080 (Torrelles *et al.* 1983) suggests that the density of this cloud is $< 5 \times 10^3$ cm^{-3}, and thus thermalization of CO by collisions is not necessarily present. Using a formalism similar to that described by Goldsmith (1972) we present in Figure 7 the values of R_2 as a function of kinetic temperature and molecular hydrogen density for an optically thin gas. As it can be seen in this figure, even for moderately high molecular hydrogen densities ($\sim 10^3$ cm^{-3}) the values of R_2 are much lower than those obtained under thermalization. Thus, low R_2 values for the high-velocity gas do not rule out the possibility of it being optically thin and hot.

Another argument that has been used to argue in favor of optically thick CO wing emission is that the T_R(CO)/T_R(^{13}CO) ratio reaches values of only ~ 20 at the extremes of the moderate velocity range over which ^{13}CO is detectable. For CO/^{13}CO abundance ratios in the range 40–89, the above ratio

TABLE 3

PARAMETERS OF THE OUTFLOWS ASSOCIATED WITH LkHα 198 AND MWC 1080

Parameter	LkHα 198	MWC 1080
Mass ($M_\odot$)	1.5	1.0×10^2
Mass rate ($M_\odot$ yr^{-1})	3.2×10^{-6}	2.6×10^{-4}
Momentum ($M_\odot$ km s^{-1})	2.6	5.5×10^2
Momentum rate ($M_\odot$ km s^{-1} yr^{-1})	6.9×10^{-6}	1.6×10^{-3}
Kinetic energy [$M_\odot$ (km s^{-1})^2]	2.8	1.8×10^3
Kinetic energy rate [$M_\odot$ (km s^{-1})^2 yr^{-1}]	8.5×10^{-6}	5.8×10^{-3}

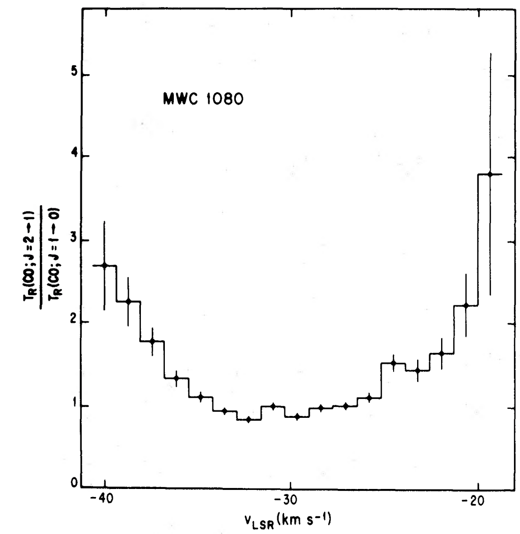

FIG. 6.—Ratio of the $J = 2 \rightarrow 1$ to $J = 1 \rightarrow 0$ source radiation temperatures for CO as a function of radial velocity with respect to the LSR for MWC 1080. Velocity resolution is 1.3 km s^{-1}. The error bar on each channel is the $\pm 1\ \sigma$ uncertainty in the ratio.

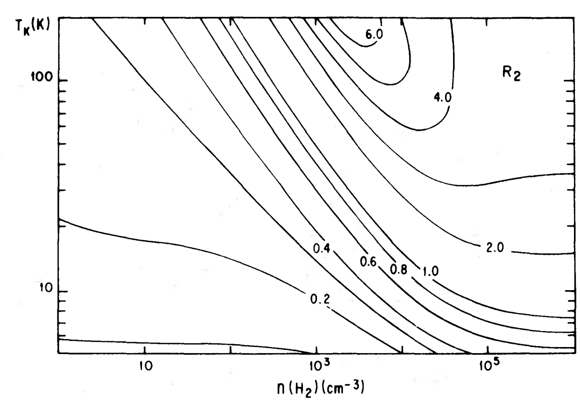

FIG. 7.—Theoretical ratio of the $J = 2 \rightarrow 1$ to $J = 1 \rightarrow 0$ source radiation temperatures for CO as a function of kinetic temperature and molecular hydrogen density for optically thin gas. Note that for cool ($T_K \lesssim 100$ K) gas with molecular hydrogen densities below $\sim 10^5$ cm^{-3} the expected ratio is smaller than the ratio under thermalization. On the other hand, ratios greater than 4 (the limit for high-temperature, optically thin, thermalized gas) are obtained for hot ($T_K \gtrsim 100$ K) gas with moderate (10^3–10^4 cm^{-3}) molecular hydrogen densities. These large values are due to the weak maser effects discussed by Goldsmith (1972).

implies moderate optical depths for the CO, $J = 1 \rightarrow 0$ transition. However, some authors (Barral and Cantó 1981; Königl 1982) have suggested that high-velocity molecular outflows are the result of steep pressure (density) gradients around the wind source. In this view the gas participating in the molecular outflow is that of the low-density medium surrounding the high-density focusing cloud. On the other hand, we know (Langer *et al.* 1980; Penzias 1983) that ^{13}CO abundance may be enhanced substantially (compared with more typical ratios) in the outer parts of molecular clouds. Thus we cannot rule out the possibility that the ^{13}CO could be enhanced by a sizable factor in the molecular outflow gas. Therefore, if this speculative enhancement is present in the high-velocity gas, one could account for the T_R(CO)/T_R(^{13}CO) ratios of $\sim$20 in terms of an optically thin source.

If one assumes that the high-velocity gas is optically thin, of constant density, and nonthermalized, Figure 7 indicates that the higher the radial velocity of the gas, the larger its temperature. For $R_2 \approx 2.5$–3 in the extreme wings, a lower limit for the kinetic temperature of $\sim$20–30 K is obtained.

Finally, we should mention that small relative pointing errors in the 2–1 and 1–0 data could lead to discrepancies in the determinations of R_2.

IV. DISCUSSION

We have observed 11 Ae and Be stars associated with nebulosity, out of which two stars show clear evidence that they are affecting with their winds the molecular environment. LkHα 198 shows a low-velocity bipolar outflow, while MWC 1080 is a case of a stellar wind affecting a considerable fraction of the cloud in which the star is embedded.

The stars where we found associated molecular motions are expected to be the youngest and/or to have the strongest winds in the sample, according to the current ideas on the origin of molecular outflows. There are a number of indications in this sense. For instance, the strength of the emission spectrum has been associated with the degree of activity and the youth in T Tauri stars (CK), and similar arguments can be made for related types of objects, such as Herbig's Be and Ae stars. Herbig (1960) divides the stars in his list into two groups of strong and weak lines; MWC 1980 is included in the former. Moreover, the spectrum of MWC 1080 by CK differs from that of the most extreme T Tauri stars only in the He I lines, which appear in absorption in this star. The emission line spectra of LkHα 198 in CK is not as rich as that of MWC 1080. Still, it has emission in the Balmer lines, and Cohen (1975) reported it as "veiled," indicating that at least in Cohen's observations the star showed a large degree of activity. On the other hand, most of the remaining stars in our sample have a weak-line spectrum.

Cohen and Schwartz (1976) define a parameter r as the ratio of the unreddened flux for $\lambda \geq 0.90\ \mu$m to that for $\lambda \leq 0.90\ \mu$m. This parameter is a measure of the amount of stellar flux emitted at infrared wavelengths and is, to first approximation, related to the presence of circumstellar material, since stars located in the same cloud show a large range of values for the parameter. Cohen and Schwartz (1976) argue that the parameter r is related to the youth of the star, in that stars that show larger r are more likely to be still surrounded by the material out of which they formed. It is therefore interesting to search for a correlation between this parameter and the presence of high velocity molecular outflows. In Table 4 we give r for the stars observed in CO. We have taken the data from Cohen and Schwartz (1976), when available. Otherwise, we have calculated it from published optical and infrared colors (Cohen 1975). We find that the two stars with associated CO outflows have the largest values of r in the sample. In this regard, it is interesting to notice that two other stars for which associated CO outflows have been clearly found, namely R Mon (Cantó *et al.* 1981) and HL Tau (Calvet, Cantó, and Rodríguez 1983), also have large values for the parameter r; 97 and 83, respectively (Cohen and Schwartz 1978). Therefore, we can conclude that there is a correlation between the presence of powerful stellar winds and circumstellar material. There are at least two possible explanations for this correlation. First, that the circumstellar material is the cause of the wind (for instance by the deposition of energy into the star's surface by accretion) or that the wind is dusty and is itself the circumstellar material. The second possibility is that circumstellar material and wind are not directly related in any way, but that they exist simultaneously during some evolutionary stage of the source, for instance during its youth.

TABLE 4

PARAMETERS RELATED TO THE PRESENCE OF CIRCUMSTELLAR MATERIAL

Star	r[a]	A_v^{op}/A_v^{CO} [a]	⟨Pol⟩[b] (%)
LkHα 198	70	1.3	...
AB Aur	1	0.6	...
RR Tau	9	0.7	...
HD 250550	10	0.04	1.7
LkHα 208	11	0.2	4.1
Z CMa	18	1.5	1.4
HD 53367	...	0.4	...
MWC 297	...	...	...
BD +40°4124	7	0.4	...
LkHα 233	21	1.2	...
MWC 1080	32	1.5	3.5

[a] See discussion in § V.

[b] From Garrison and Anderson 1978. Values are corrected for interstellar polarization.

Another indication that the stars with CO outflows are still surrounded by material left over from the accretion process comes from the ratio of the extinctions determined from the optical spectra, A_v^{op}, to the amount of molecular material located along the line of sight, A_v^{CO}. This ratio is expected to be correlated with the circumstellar extinction and is given in Table 4 for the observed stars. Although there is large uncertainty in the determination of this ratio, especially in A_v^{op}, it is suggestive that LkHα 198 and MWC 1080 consistently have $A_v^{op}/A_v^{CO} > 1$. Additional indications come from polarization measurements. Table 4 gives the mean of the polarization degree in the continuum for the few stars in our sample where it has been reported (Garrison and Anderson 1978). MWC 1080 has one of the largest polarizations, indicative of the presence of a dust distribution around the star, if the polarization is interpreted in terms of the same model as for T Tauri stars (Bastien 1982). Similarly, one should mention that R Mon and HL Tau have very large polarizations, 15% and 8.3%, respectively (Garrison and Anderson 1978; Bastien 1982).

We now return to what was originally the main purpose of this paper, namely, to find more cases of young stars of intermediate luminosity ($10^2 \leq L/L_\odot \leq 10^3$) associated with molecular outflows. The sources discussed by Bally and Lada (1983) contain only two examples: NGC 2071 and HH 24 – 26. Since both LkHα 198 and MWC 1080 have been assigned spectral types of early B similar to those of obscured objects within molecular outflows (Rodríguez *et al.* 1982; Bally and Lada 1983), we conclude that we did not find in our sample a conclusive case of such an intermediate-luminosity star with a CO outflow. However, it should be noted that the spectral types of LkHα 198 and specially that of MWC 1080 may be in error. The spectral classification of CK for early types is based on the strength of the He I absorption lines, which are not very reliable indicators (J. L. Linsky, private communication). The classification is specially uncertain in the case of MWC 1080, a star with a large degree of activity. MWC 1080 has a spectrum very similar to that of R Mon (CK), which has also classified as a B0 by these authors. However, assuming for R Mon a distance of 700 pc (Cantó *et al.* 1981) and L/D^2 as given by CK, one obtains a luminosity that would put the star well below the main sequence if a B0 type is adopted. A spectrum taken by Mendoza (1970) indicates a type of A5 for R Mon, which is a much more reasonable estimate. We have no information for MWC 1080 other than that provided by CK's low resolution spectra. However, in analogy to R Mon, we suspect that a spectral type later than B0 would be more appropriate.

The spectral classification for LkHα 198 may not be in a large error, since the stellar spectrum is not so strongly "veiled" in CK as that of MWC 1080.

V. CONCLUSIONS

We observed carbon monoxide emission from the molecular surroundings of 11 Herbig Be- and Ae-type stars searching for peculiar motions that could be attributed to a stellar wind interacting with the associated cloud. Our main conclusions can be summarized as follows:

1. Although several of the clouds observed show evidence of localized heating and peculiar kinematics, only those associated with LkHα 198 and MWC 1080 show clear evidence of molecular outflows.
2. The outflow associated with LkHα 198 appears to be bipolar and is of moderate radial velocity.
3. The outflow related to MWC 1080 is very powerful; we estimate a mass loss rate of $\dot{M} \approx 10^{-5}\ M_\odot\ \mathrm{yr}^{-1}$ for this star. As in most of the molecular outflows, the momentum rate injected into the cloud significantly exceeds the radiative momentum rate available in stellar photons.
4. There are several evidences pointing to a correlation between abundant circumstellar material and detectable molecular outflows. In particular, the parameter r (Cohen and Schwartz 1976) is very high for sources with CO outflows.
5. In our sample, we did not find a conclusive case of an intermediate-luminosity star with a CO outflow.

We acknowledge the help of Rosalie Douglas and Calvin Sparks during the observing run at Kitt Peak and of J. F. Barral in the preparation of Figure 7. J. C. and L. F. R. acknowledge partial support of CONACYT (Mexico) grant PCCBBEU-020510 and R. M. L. the support of NSF grant AST 81-16403.

REFERENCES

Bally, J., and Lada, C. J. 1983, *Ap. J.*, **265**, 824.
Bally, J., and Scoville, N. Z. 1982, *Ap. J.*, **255**, 497.
Barral, J. F., and Cantó, J. 1981, *Rev. Mexicana Astr. Ap.*, **5**, 101.
Bastien, P. 1982, *Astr. Ap. Suppl.*, **48**, 159.
Calvet, N., and Cohen, M. 1978, *M.N.R.A.S.*, **182**, 687.
Calvet, N., Cantó, J., and Rodríguez, L. F. 1983, *Ap. J.*, **268**, 739.
Cantó, J., Rodríguez, L. F., Barral, J. F., and Carral, P. 1981, *Ap. J.*, **244**, 102.
Cohen, M. 1975, *M.N.R.A.S.*, **173**, 279.
Cohen, M., and Kuhi, L. V. 1979, *Ap. J. Suppl.*, **41**, 743 (CK).
Cohen, M., and Schwartz, R. D. 1976, *M.N.R.A.S.*, **174**, 137.
Cova, J., Della Prugna, F., Araque, M. C., and Calvet, N. 1984, in preparation.
Della Prugna, F. 1982, private communication.
Dickman, R. L. 1978, *Ap. J. Suppl.*, **37**, 407.
Edwards, S., and Snell, R. L. 1982, *Ap. J.*, **261**, 151.
Elias, J. H. 1978, *Ap. J.*, **224**, 857.
Felenbock, P., Praderie, F., and Talavera, A. 1983, *Astr. Ap.*, submitted.
Finkenzeller, U., and Mundt, R. 1984, *Astr. Ap. Suppl.*, **55**, 109.
Fitzgerald, M. P. 1968, *A.J.*, **73**, 983.
Garrison, L. M. 1978, *Ap. J.*, **224**, 535.
Garrison, L. M., and Anderson, C. M. 1977, *Ap. J.*, **218**, 438.
———. 1978, *Ap. J.*, **221**, 601.
Gerola, H., Salem, M., and Panagia, N. 1971, *Ap. Space Sci.*, **10**, 383.
Goldsmith, P. F. 1972, *Ap. J.*, **176**, 597.
Goldsmith, P. F., and Langer, W. D. 1978, *Ap. J.*, **222**, 881.
Herbig, G. H. 1954, *Trans. IAU*, **8**, 805.
———. 1960, *Ap. J. Suppl.*, **6**, 337.
Herbst, W., Racine, R., and Warner, J. W. 1978, *Ap. J.*, **223**, 471.
Hubert-Deplace, A. M., and Hubert, H. 1979, *An Atlas of Be Stars* (Paris: Meudon Observatory).
Königl, A. 1982, *Ap. J.*, **261**, 115.
Kutner, M. L., Leung, C. M., Machnik, D. E., and Mead, K. N. 1982, *Ap. J. (Letters)*, **259**, L35.
Kutner, M. L., and Ulich, B. L. 1981, *Ap. J.*, **250**, 341.
Kwan, J., and Scoville, N. 1976, *Ap. J. (Letters)*, **210**, L39.
Langer, W. D., Goldsmith, P. F., Carlson, E. R., and Wilson, R. W. 1980, *Ap. J. (Letters)*, **235**, L39.
Levreault, R. M. 1983, *Ap. J.*, **265**, 855.
Little, L. T., MacDonald, G. H., Riley, P. W., and Matheson, D. N. 1979, *M.N.R.A.S.*, **188**, 429.
Loren, R. B. 1977, *Ap. J.*, **218**, 716.
Loren, R. B., Plambeck, R. L., Davis, J. H., and Snell, R. L. 1981, *Ap. J.*, **245**, 495.
Loren, R. B., Vanden Bout, P. A., and Davis, J. H. 1973, *Ap. J. (Letters)*, **185**, L67.
Loren, R. B., and Wootten, H. A. 1978, *Ap. J. (Letters)*, **225**, L81.
Marlborough, J. M. 1970, *Ap. J.*, **159**, 575.
Mendoza V, E. E. 1970, *Mém. Soc. Roy. Sci. Liège*, 5e Sèr., **19**, 319.
Panagia, N. 1973, *A.J.*, **78**, 929.
Penzias, A. A. 1983, *Ap. J.*, **273**, 195.
Plambeck, R. L., Snell, R. L., and Loren, R. B. 1983, *Ap. J.*, **266**, 321.
Rodríguez, L. F., Carral, P., Ho, P. T. P., and Moran, J. M. 1982, *Ap. J.*, **260**, 635.
Schuster, W. J. 1984, in preparation.
Strom, S. E., Strom, K. M., Yost, J., Carrasco, L., and Grasdalen, G. 1972, *Ap. J.*, **173**, 353.
Torrelles, J. M., *et al.* 1983, *Ap. J.*, **274**, 214.
Ulich, B. L., and Haas, R. W. 1976, *Ap. J. Suppl.*, **30**, 247.
Zuckerman, B., Kuiper, T. B. H., and Rodríguez Kuiper, E. H. 1976, *Ap. J. (Letters)*, **209**, L137.

N. Calvet: Centro de Investigación de Astronomía "Francisco J. Duarte," Apartado 264, Mérida, Venezuela

J. Cantó and L. F. Rodríguez: Instituto de Astronomía, Universidad Nacional Autónoma de México, Apdo. Postal 70-264, C.U., 04510 México, D.F. México

R. M. Levreault: Department of Astronomy, University of Texas at Austin, Austin, TX 78712